17th Brazilian Congress of Thermal Sciences and Engineering
November 25th-28th, 2018, Águas de Lindóia, SP, Brazil

ENCIT 2018
EXPERIMENTAL ANALYSIS OF THE START-UP FLOW OF VISCOUS AND VISCOPLASTIC FLUIDS IN PIPELINES

Lucas Garcia Pereira
lucper.2016@alunos.utfpr.edu.br

Airton David Filho
airtonfilho@alunos.utfpr.edu.br

Diogo Elias da Vinha Andrade
diogoandrade@utfpr.edu.br

Tainan Gabardo Miranda dos Santos
tainansantos@utfpr.edu.br

Cezar Otaviano Ribeiro Negrão
negrao@utfpr.edu.br

Research Center for Rheology and Non-Newtonian Fluids (CERNN)
Postgraduate Program in Mechanical and Materials Engineering (PPGEM)
Federal University of Technology – Paraná (UTFPR)
R. Deputado Heitor Alencar Furtado, 5000, CEP: 81280-340 Curitiba-PR-Brazil.

Abstract. *Waxy oils can cause many problems to the petroleum industry, such as production losses and pump overload. This happens due to wax crystallization in the oil, which may generate a gelled structure during production shutdowns. To restart the flow, the non-Newtonian gel requires higher pressures than the usual, which are not easily predicted by mathematical models. According to the literature, the restart pressures are influenced by the gel's yield stress and high viscosity. The objective of this paper is to better understand these parameters by studying them separately, utilizing two simpler fluids, glycerin and a water-based carbomer gel (Carbopol®). These fluids were submitted to a series of tests performed in an experimental rig, which consists of a long thermally-controlled helical pipe. The measured results will allow the correlation of the mentioned effects with the start-up pressures exhibited by the gelled waxy oil, providing a better overall comprehension of the start-up flow phenomena.*

Keywords: *gliceryn, Carbopol®, experimental rig, flow start-up, non-Newtonian fluid.*

1. INTRODUCTION

The offshore production of waxy crude oils is still a challenging activity. In reservoir conditions (average temperature of 80 °C), the oil behaves as a Newtonian fluid. However during the transportation, through pipelines placed on the seabed, the crude oil cools down due to heat exchanges with the cold water (average temperature of 4 °C) (Vieira, 2008). Because of the cooling, paraffin crystals precipitate in the oil providing a non-Newtonian behavior on the material (Azevedo and Teixeira, 2003). Moreover, these crystals tend to deposit at the inner walls of the pipeline and increase the viscosity of the oil (Sanjay *et al*., 1995; Wardhaugh and Boger, 1987). As the paraffin precipitation continues, the crystals may also build up a gelled structure in the oil, which mainly occurs during maintenance and emergency shutdowns (Davidson *et al*., 2004). These phenomena involving paraffin precipitation and subsequently deposition are very onerous to the oil and gas industry, causing flow rate reduction, equipment failure and eventually blocking the pipeline (Sanjay *et al*., 1995). Even recently, hundreds of millions of dollars are spent every year to mitigate and solve these operational problems, as reported by Bagdat and Masoud (2015).

A decrease in the production is also noticed in the case where the gelled structured is generated (Hénaut *et al*., 1999). In order to restart the flow, pressures higher than the usual steady state one are required to break the gelled structure (Wardhaugh and Boger, 1987).

Therefore, it is important to understand the parameters that influence on the restart pressure profile and its magnitude, because the overestimation of this pressure could lead to oversized pipeline projects, which are unviable for application (Fossen *et al*., 2013).

As mentioned before, these materials exhibit a complex non-Newtonian behavior, whose properties depend not only on its chemical composition, but also on the shear and thermal histories faced by the oil (Marchesini *et al.*, 2012). In the gelled form, the material is usually modeled as an elasto-viscoplastic material with a viscosity dependent of the time and the applied shear rate (Tarcha *et al.*, 2015). Besides, some mathematical models also account the compressibility of the material as a relevant variable to predict the flow restart in pipelines (Ahmadpour and Sadeghy, 2014; Cawkwell and Charles, 1987; Oliveira and Negrão, 2015; Vinay *et al.*, 2006). This is also suggested by some papers which study the problem by means of experimental rigs (Borghi *et al.*, 2003; Lee *et al.*, 2008; El-Gendy *et al.*, 2012; Magda *et al.*, 2013), in order to relate the gel breaking mechanism with the pressure propagation and compressibility of the material.

With so many effects acting simultaneously in the waxy oil, it is important to study them individually in order to verify their relevance and improve future mathematical models. This can be done with experimental rigs, which conditions are more similar than the observed in the field. Therefore, this works aim to experimentally evaluate the effects of viscosity, viscoplasticity and compressibility on start-up flows of time dependent fluids (such as gelled waxy oils) in pipelines, by measuring the pressure in a long thermally-controlled helical pipe, for different materials and two flow conditions.

2. METHODOLOGY

In order to conduct this study, an experimental rig was used to control the flow rate, the inlet pressure and the temperature of two simpler fluids (Newtonian and viscoplastic) within a long pipeline inside a temperature controlled chamber. Several tests were performed to each fluid, in order to better understand the effects and attempt to correlate them to the behavior present in the gelled waxy oil.

2.1 Working fluids

To study the viscous effects, a sample of bidistilled glycerin was used, because this material usually behaves as a Newtonian fluid and exhibits substantial changes in the viscosity with temperature (Takamura *et al.*, 2012). The effects of the yield stress (viscoplasticity) were evaluated through tests performed with a water-based carbomer gel (Carbopol®), as this gel behaves like an ideal viscoplastic fluid (Balmforth *et al.*, 2014). The viscoplastic material is composed by 96% ultrasound gel and 4% biocide (v/v concentration).

2.2 Experimental rig

The experimental rig used consists of two syringe pumps connected to a long helical pipeline, on which are installed absolute pressure transducers and several uniform-spaced thermocouples. The whole set is within a large thermally insulated chamber, to provide a controlled temperature during the tests. The flow loop used for the experiments is shown schematically in Figure 1.

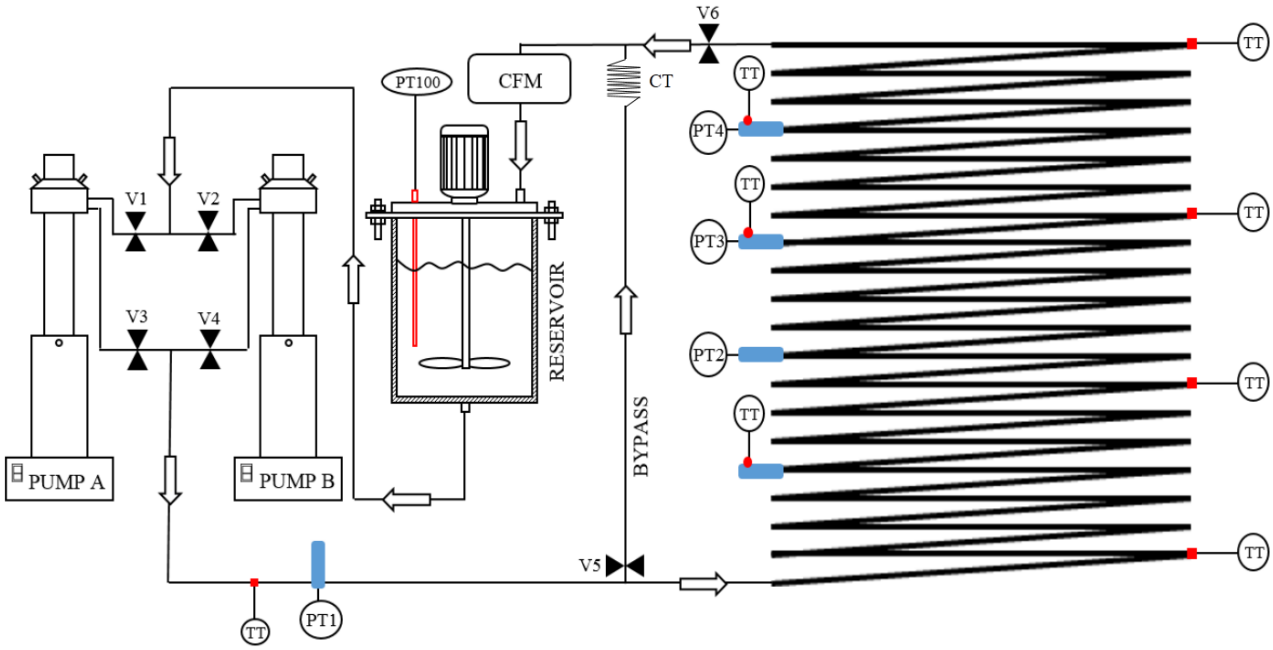

Figure 1. Schematic diagram of the experimental rig and its components

Two syringe pumps manufactured by Teledyne ISCO™, model 500D, provide the flow to the pipeline. This equipment can reach up to 250 bar, providing a flow rate ranging from 0.001 ml/min to a maximum of 204 ml/min. Depending on the flow specified by an external controller, the set of pumps work separately or simultaneously. The external controller drives pneumatically the ball valves V1, V2, V3 and V4 in order to regulate the operation. Both devices have an accuracy of ± 0.5% for the flow rate.

The helical pipe has 50.53 meters length and an inner diameter around 10.0 mm. A bypass line is installed before the helical pipe as a shortcut between the entrance and exit of the helical pipe. This bypass has a capillary tube (CT) of inner diameter of 2.03 mm and 1.2 meters length, which allows the imposition of higher pressures on the pipeline.

The flow path along the pipeline (represented by the arrows) is controlled by ball valves (V5 and V6) which are driven pneumatically. By the end of the pipeline, a Micro Motion® Coriolis flow and density meter (CFM) obtains instant values of flow rate and density, before leading the fluid back to the hermetically sealed reservoir.

The absolute pressure transducers are manufactured by HBM™, model P3 Industrial Class, their maximum allowed pressures are 20 bar, and they all have an internal resistance thermometer (RTD) installed. Transducer PT1 is assembled immediately after the pumps, to measure the inlet pressure, PT2, PT3 and PT4 are, respectively, distant 21.74, 32.77 and 43.87 m from PT1. After PT4, there are extra 8.63 meters of pipeline, which leads to V6. The accuracy of all pressure transducers is 0.03 bar.

The temperatures are measured with eight thermocouples (TT) along the pipeline surface and one RTD (PT100) inside the reservoir, and are converted to analog signals. These signals are gathered by the acquisition system, and sent to the LabVIEW 2016™ software, which also works as the main interface to follow up and verify other variables of the system, such as pressure and elapsed time. The software runs a PID controller that manages to make the chamber achieve and maintain the desired average temperature for the tests, by compensating the operation of a set of electrical resistances and a refrigeration unit. The maximum standard deviation of the steady state measured temperatures was 0.29 °C, being the average value the desired one. Based on that fact, the control system of the experimental rig can be considered effective to apply and maintain a uniform temperature distribution along the apparatus.

It is important to notice that, considering the maximum flow rate provided by the pumps, the high viscosity of the fluid and the inner diameter of the pipeline, all the flows generated by the experimental rig will remain laminar.

2.3 Experimental procedures

The present paper intends to execute three tests in two different temperatures. Every test was performed three times to assure repeatability, and no significant variance was verified among each repetition. The flow start-up tests with glycerin were executed at 25 and 45 °C. In the case of the Carbopol® gel, 5 and 25 °C.

For all the experiments, the first step is to achieve the test temperature inside the chamber. After temperature distribution is uniform along the pipeline, 30 minutes are waited to guarantee that the fluid within the pipe has the same temperature as its surface, which can be confirmed by the RTD of the pressure transducers. After that, valves V1, V2, V3, V4 and V6 are opened and 3 minutes are waited, so the pressure transducers can achieve an initial pressure distribution that is the same for every experimental procedure.

a) Pressure transmission

It is very important to verify if the material fully transmits the imposed pressure, since many mathematical models relate the flow start-up to the pressure wave propagation (Ahmadpour and Sadeghy, 2014; Kumar *et al*., 2015; Oliveira and Negrão, 2015). This test evaluates the pressure transmission by simply setting a flow rate and allowing the material flow through the bypass (V5 open, V6 closed), and then monitoring the pressures evolution on all transducers, until the steady state value. If the material fully transmits the pressure, P2, P3 and P4 will have the same value.

b) Flow start-up with inlet constant flow rate

This procedure is done with V6 opened and V5 closed, allowing the fluid to flow only through the helical pipe. Then the desired flow rate must be set up to the pumps, and after the start-up, the pressure profile is recorded until the pressures reach equilibrium. The selected flow rates are 0.064, 0.644, 6.44, 32.2, 64.4 and 128.8 ml/min. These values correspond to shear rates of approximately 0.01, 0.1, 1, 5, 10 and 20 s^{-1}, for a Newtonian fluid, respectively. The results obtained in this test can be used to estimate a flow curve, utilizing the following equations:

$$\tau_w = \frac{D\Delta P}{4L} \tag{1}$$

$$\dot{\gamma}_w = \frac{32Q}{\pi D^3} \tag{2}$$

$$\dot{\gamma}_{wr} = \frac{\dot{\gamma}_w}{4}\left(3 + \frac{d\ln Q}{d\ln \tau_w}\right) \tag{3}$$

In Equation (1), τ_w is the wall shear stress, D the inner diameter, ΔP the pressure difference between PT1 and PT4 (P1 – P4), L the distance between PT1 and PT4. In Equation (2), $\dot{\gamma}_w$ is the wall shear rate for Newtonian fluids and Q the volumetric flow rate. Equation (3), known as Weissenberg-Rabinowitsch equation, is used to calculate the wall shear rate ($\dot{\gamma}_{wr}$) for pressure driven flows (Macosko, 1994).

3. RESULTS AND DISCUSSION

3.1 Flow curve

The flow curves and their fits for both materials is shown in Figure 2. The data concerning the shear stresses were evaluated at steady state.

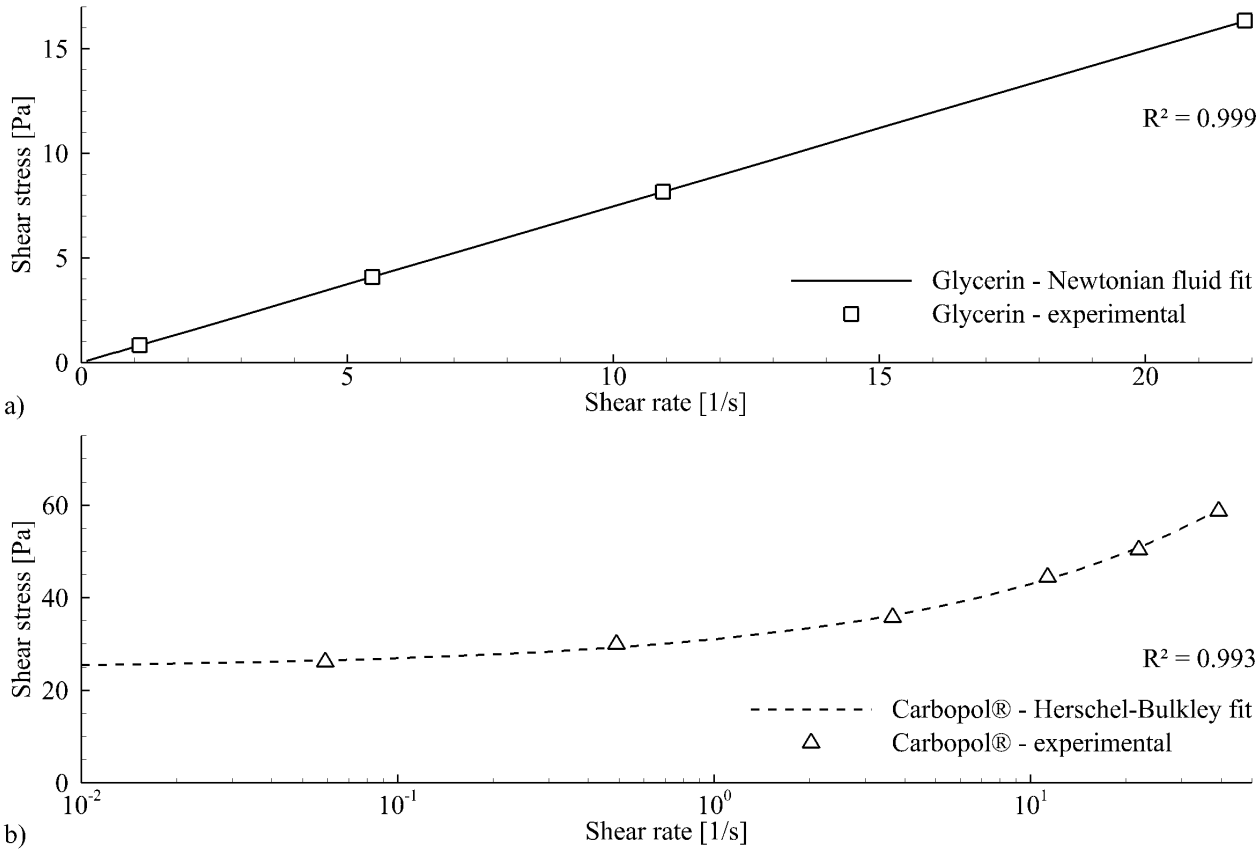

Figure 2. Flow curves for (a) glycerin and (b) Carbopol®, with flow rates of 0.064, 0.644, 6.44, 32.2, 64.4 and 128.8 ml/min

Figure 2 (a) presents the experimental flow curve for glycerin, which matches the behavior for a Newtonian fluid. wo points were removed from this flow curve, corresponding to 0.644 ml/min and 0.064 ml/min. The flow rate of 0.664 ml/min generated a very low ΔP, which was within the transducer's accuracy range. The lowest flow rate (0.064 ml/min) did not result in any pressure difference and was also not used. The remaining values resulted in a flow curve that can be expressed as: $\tau_w = 0.7464\dot{\gamma}_w$, with a maximum deviation of 0.51%, for 6.44 ml/min, which can be expected since, considering this experimental apparatus, lower pressures generate higher experimental uncertainties. The adjusted line perfectly fitted the experimental data, with a coefficient of determination of 0.999.

The viscoplastic material, presented in Figure 2 (b), exhibited changes in viscosity with shear rate, as we can see in the flow curve, being pseudoplastic. For such case, the Herschel-Bulkley equation was used to fit the experimental data, resulting in the following expression: $\tau_w = 24.7 + 6.3\dot{\gamma}_{rw}^{0.46}$. The deviation between the experimental and the fitted data is within a range of 2.5% and a coefficient of determination of 0.993, indicating a good adjustment.

3.2 Pressure transmission

Figure 3 (a) and (b) presents the results for glycerin and Carbopol® at 25 °C, with flow rates of 42.3 ml/min and 64.4 ml/min, respectively. In both cases, after the initial condition is achieved, the pumps are turned on and all the pressure are recorded until they reach steady state.

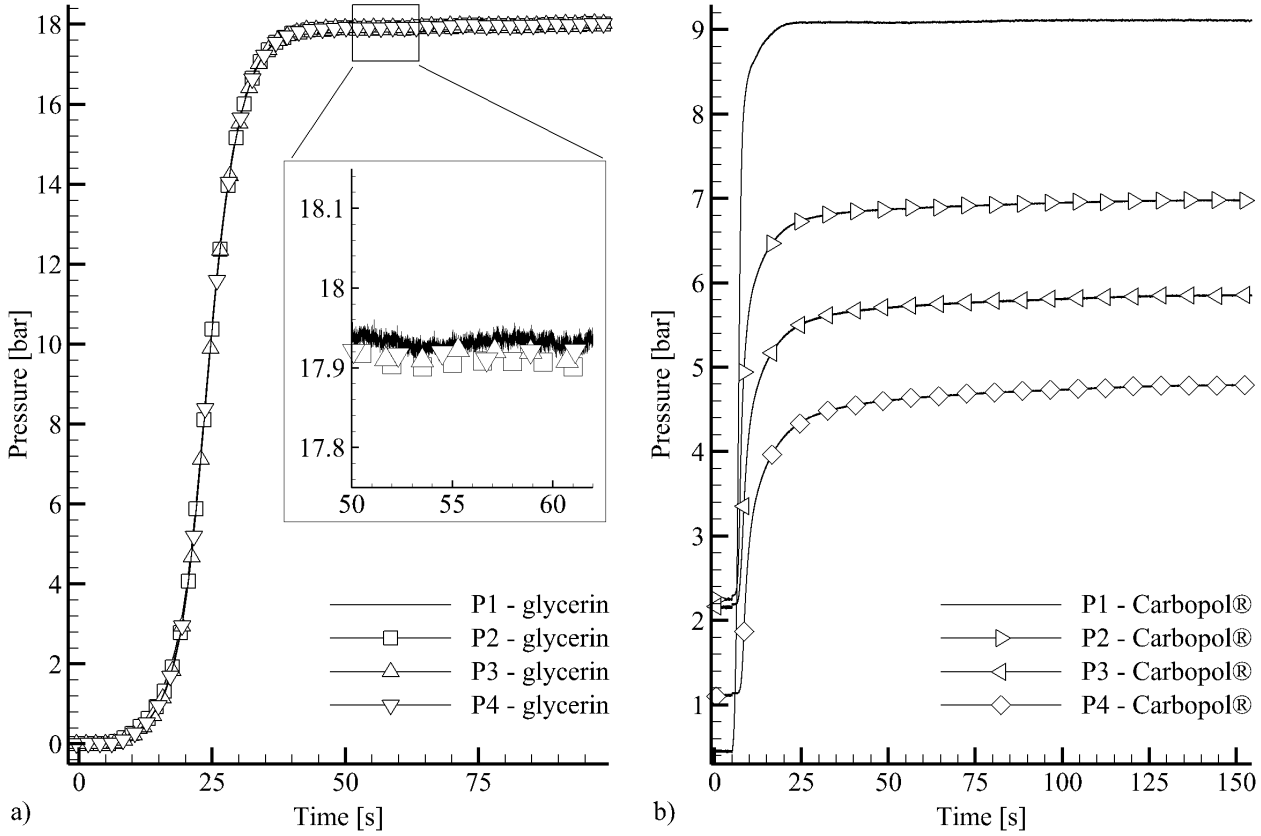

Figure 3. Pressure transmission test at 25 °C. (a) glycerin at 42.3 ml/min and (b) Carbopol® at 80.5 ml/min

Before the pumps are turned on, it can be noted that the initial pressure distribution is different for each fluid, which already indicates that the carbomer gel does not fully transmits pressure. In Figure 3 (a), the initial pressure is 0 bar for every transducer, at 5 seconds the pumps are turned on and the glycerin flows through the bypass, progressively pressurizing the whole pipeline to around 17.90 bar at 45 s. The inset shows the final pressure distribution between 50 and 60 seconds, with average values of 17.94 bar at PT1 and 17.92 at PT2, PT3 and PT4. P1 is slightly higher than P2, P3 and P4, due to the position of the first transducer, which is before the bypass. It can also be noted some oscillation on the steady state values of P1 but this behavior is followed by the other transducers, confirming that the fluid transmits pressure. This oscillation could be caused due to temperature variations or small heterogeneities in the material. Throughout the whole test, the average difference among P2, P3 and P4 was insignificant and within the transducer's accuracy range, therefore this material fully transmits pressure.

Figure 3 (b) shows P1 starting at 0.45 bar, P2 2.25 bar, P3 at 2.15 bar and P4 1.11 bar, which is due to the position of each transducer and the non-transmissibility of pressure. PT1 is the closest to the reservoir (atmospheric pressure), so it measures the lowest pressure. As PT2 and PT3 are placed from almost the same distance from the reservoir, P2 and P3 are similar. PT4 is around 10 meters far from the reservoir, so it's residual pressure is higher than P1.

During the test, after the pumping starts (also at 5 seconds), P1 immediately starts to increase, followed by P2, P3 and P4. The pressure on the first transducer reaches equilibrium at 21 seconds, measuring 9.11 bar. The increase on P2, P3 and P4 slows down during the procedure, eventually reaching steady state at the end of the test. This result confirms that for the current time scale, the carbomer gel does not transmit the applied pressure. The final pressure distribution is

P1 = 9.11 bar; P2 = 6.98 bar; P3 = 5.85 bar and P4 = 4.79 bar, resulting in a shear stress of around 24.6 Pa at the pipe's wall. This is an interesting result if compared with the yield stress fitted by the Herschel-Bulkley equation on the previous test (24.7 Pa). These values are very much alike each other, which may indicate a relation between viscoplasiciy and the non-transmission of pressure exhibited by the material.

3.3 Flow start-up with inlet flow rate

Figure 4 shows in details the flow start-up process for glycerin with constant 64.4 ml/min at 25 °C, including the measures taken by the flow meter. All images show the pressures development with time, from the start-up of the pumps until the flow reaches steady state.

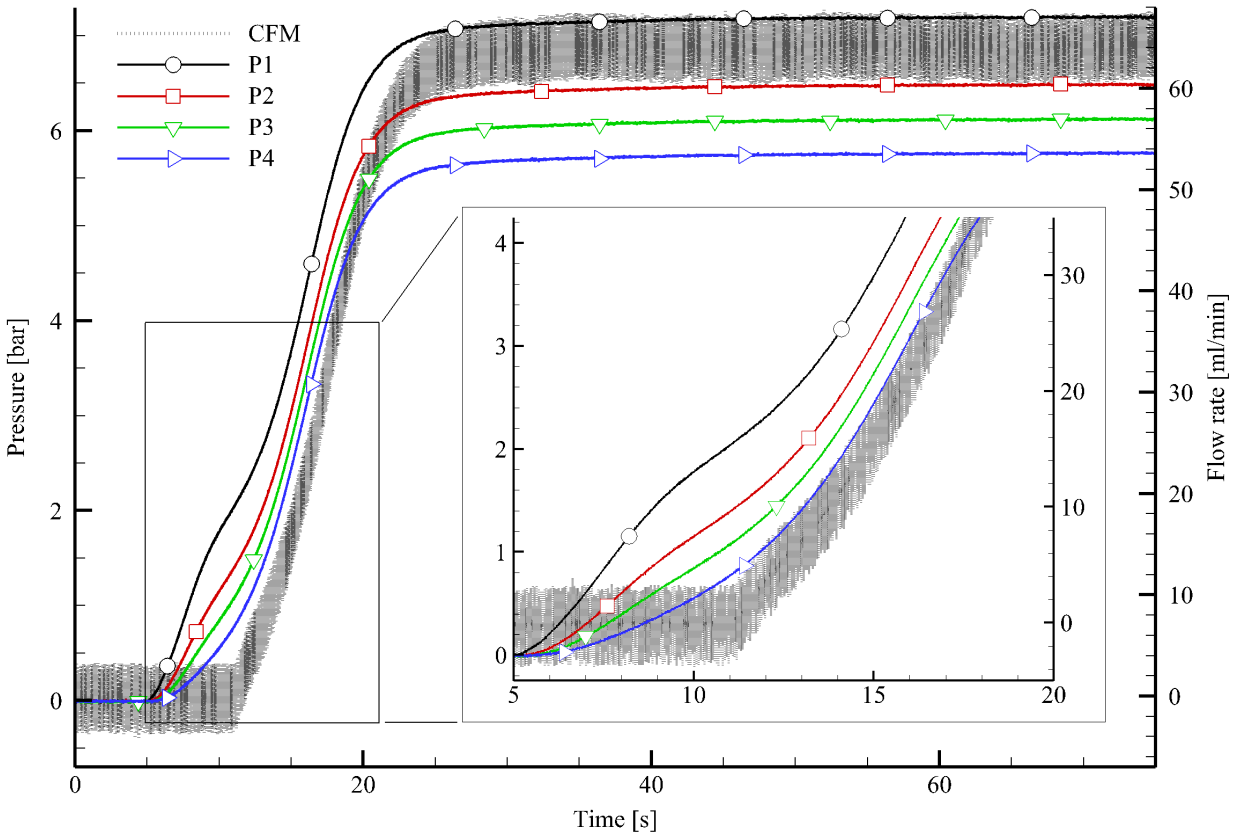

Figure 4. Glycerin flow start-up with constant flow rate of 64.4 ml/min, at 25 °C

For this test, when the pumps are activated, apparently all pressures begin to increase together, but with different velocities, reaching the equilibrium value after 31 seconds. The equilibrium pressure for P1 is 7.18 bar, followed by 6.47 bar at P2, 6.11 bar at P3 and 5.75 bar at P4. The maximum pressure difference between the transducers are proportional to the distance between them, which is coherent and expected for a Newtonian fluid. It is worth to point that the increase of P1 during the transient part of the experiment occurs in three distinct steps. The inset shows that the initial pressure growth occurs until 10 s, followed by a decrease in the pressure increase rate until it accelerates again after 15 seconds. It is believed to be due to the flow meter, which accounts for a huge part of the total head loss (more than 75%). It would also explain the fact that, after the CFM starts measuring non-zero flow rates, P4 is the first to reach an almost linear pressure increase behavior with time, followed by P3, P2 and only then P1, as their transducers are further away from the flow meter and take more time to acknowledge this huge local pressure loss.

Figure 5 presents another flow start-up with 64.4 ml/min but this time at 45 °C. The pressures achieved in this test are much lower than those achieved by the previous test, being also proportional to the apparent viscosity of the fluid. The pumps are started also at 5 seconds and the steady state was reached at around 28 seconds, which was faster compared to the previous test (31 seconds). This is also expected, since the material is less viscous and therefore less dissipative. The equilibrium values are 1.66 bar, 1.50 bar, 1.41 bar and 1.33 bar, for P1, P2, P3 and P4 respectively. The inset of Figure 5 displays the measured pressures during the initial seconds. It shows that the behavior caused by the flow meter's pressure loss is much less intense for this less viscous case, and the pressure profile is much more stable and linear during the transient stage of the test.

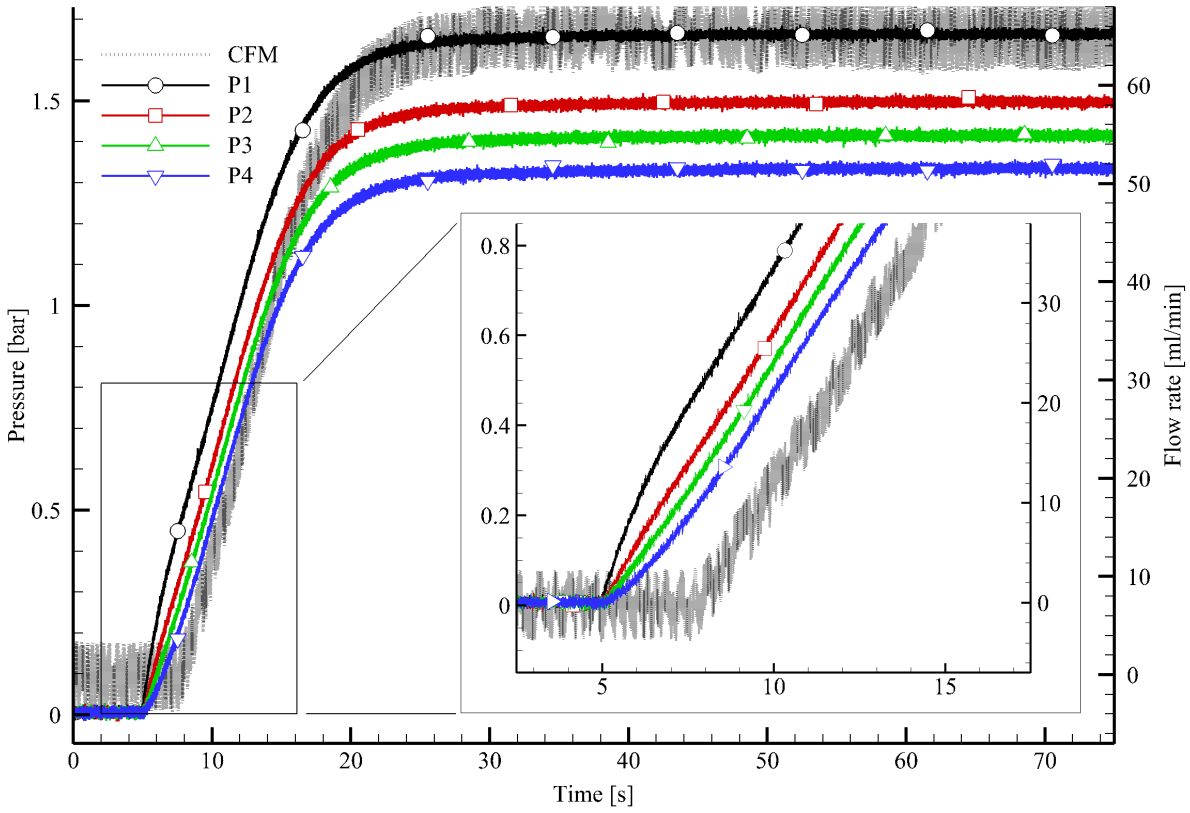

Figure 5. Glycerin flow start-up with constant flow rate of 64.4 ml/min, at 45 °C

Figure 6 presents the pressures as a function of time for the Carbopol® sample, (a) at 25 °C and (b) at 5 °C, with a constant inlet flow rate of 64.4 ml/min.

Besides the temperature difference, both curves follow the same trend. In Figure 6 (a), as the pumping begins, P1 immediately starts to increase, followed by P2 at 6.49 s, P3 at 7.21 s and P4 at around 7.85 s, resulting in a delayed time of 1.49 seconds, 2.21 seconds and 2.84 seconds from P1, respectively. This behavior is different from the glycerin, which had the pressures increasing almost at the same time, just after the start-up of the pump. During the transient phase, all transducers present a change on the pressure's increase rate, which is felt first by PT4 and lastly by PT1. This change on the pressure's profile probably happens when the material is pressurized through the CFM, considering that P4's curve tends towards steady steady immediately after the flow rate starts to rise. The trend observed on P4 is followed by P3, P2 and finally P1.

At 11 seconds, the pressures reach steady state, P1 is equal to 12.73 bar, P2, P3 and P4 are 8.56, 6.42 and 4.15, respectively. Differently from the start-up test with glycerin, in which the flow rate and the pressures stabilize at almost the same time, the equilibrium values for the CFM are achieved 3.5 seconds after the pressure values, indicating that the flow starts only after the fluid is almost fully pressurized. It is also interesting to notice that the local pressure loss caused by the CFM is much less expressive for this case than it was for the glycerin. This can be explained by the pseudoplastic behavior of the Carbopol®, which diminishes the material's viscosity while it flows through the flow meter, whose contraction promotes a high shear rate.

Figure 6 (b) shows basically the same behavior as Figure 6 (a). The main differences are the maximum pressures and the steady state time. The average values are 14.95 bar for P1, 10.02 bar for P2, 7.43 bar for P4 and 4.83 bar for P4, achieved at 12 seconds. The flow rate stabilizes at around 15.5 seconds. Those results are consistent, due to the increase in the system's dissipation with the decrease of temperature.

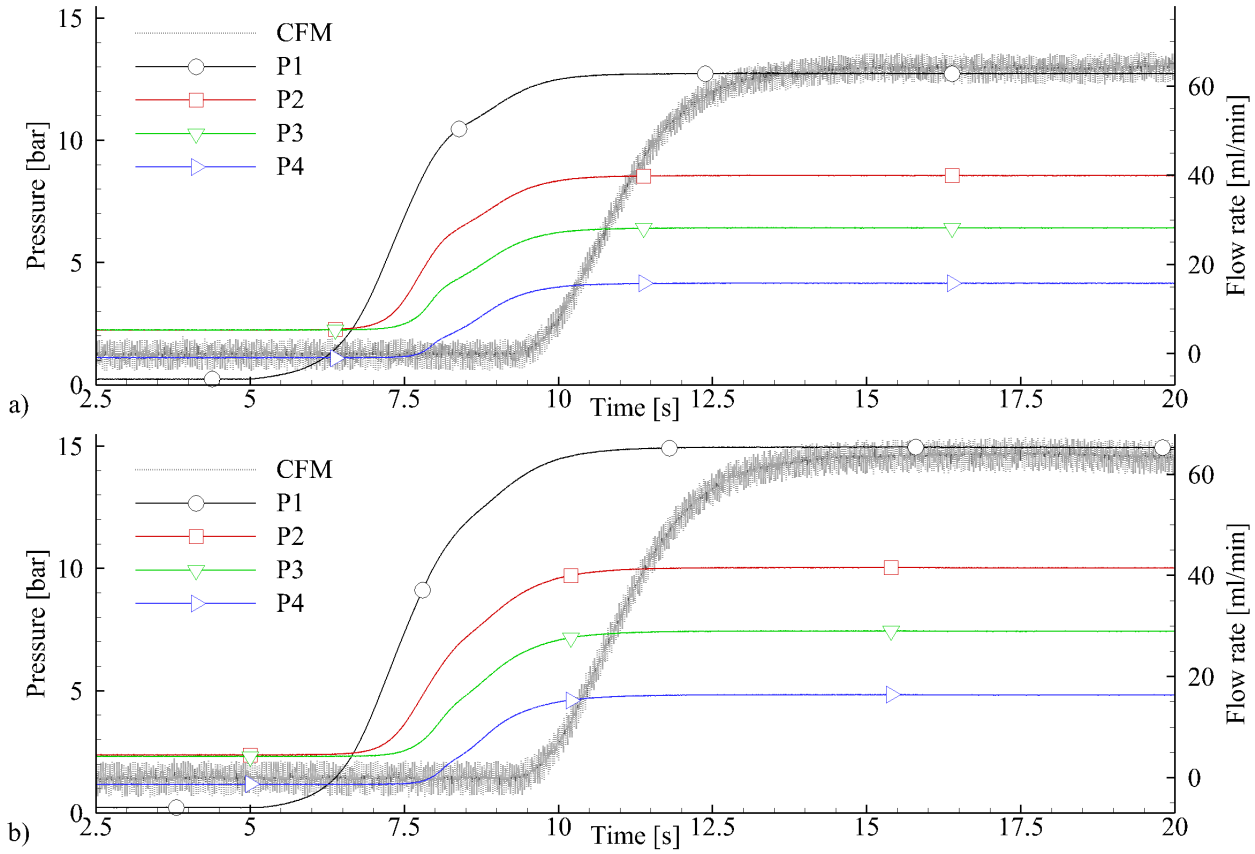

Figure 6. Carbopol® flow start-up with constant flow rate of 64.4 ml/min, (a) at 25 °C and (b) at 5 °C

4. FINAL REMARKS

This paper presented the experimental rig and the methodology to study the effects of viscosity and viscoplasticity, which are parameters that influence the start-up flow of gelled materials. The chosen fluids to evaluate these parameters were bidistilled glycerin and ultrasound gel (Carbopol®), respectively.

First, were presented the flow curves correspondent to both materials. As expected, the bidistilled glycerin showed a constant viscosity with shear rate, characterizing a Newtonian fluid. The carbomer gel exhibited not only viscoplasticity, but also pseudoplasticity, and was fitted according to the Herschel-Bulkley equation.

The pressure transmission procedures generated coherent results. It was verified that glycerin, even being a high viscosity liquid, fully transmits the applied pressure to all transducers installed in the helical pipeline. In the case of Carbopol®, the pressure transmission was not achieved, generating a residual wall shear stress very similar to the yield stress found with the Herschel-Bulkley fit, which indicates an apparent relation between these two quantities.

The flow start-up with inlet flow rate also showed very different trends for both fluids. For glycerin, the pressure in all transducers start to increase immediately after the pumping, at different rates, reaching steady state almost at the same time as the CFM. In the case of Carbopol®, it was noticed that PT2, PT3 and PT4 are delayed in comparison to PT1, and the measured flow rate at the end of the pipeline starts to increase only after the system is almost fully pressurized.

This work can be complemented by future experiments with thixotropic fluids, which may provide a better understanding of the start-up phenomena by account the time dependent effects.

5. ACKNOWLEDGEMENTS

The authors acknowledge the financial support of PETROBRAS S/A, ANP (Brazilian National Oil Agency). We also thank Eng. Nezia de Rosso for her valuable support with the experimental rig.

6. REFERENCES

Ahmadpour, Ali, and Kayvan Sadeghy. 2014. Start-up flows of Dullaert-Mewis viscoplastic-thixoelastic fluids: A two-dimensional analysis. *Journal of Non-Newtonian Fluid Mechanics* 214: 1–17.

Azevedo, L. F. A., and A. M. Teixeira. 2003. A Critical Review of the Modeling of Wax Deposition Mechanisms. *Petroleum Science and Technology* 21: 393–408.

Bagdat, Mombekov, and Rashidi Masoud. 2015. Control of Paraffn Deposition in Production Operation by Using Ethylene–TetraFluoroEthylene (ETFE). In *ICIPEG 2014*, ed. Mariyamni Awang, Berihun Mamo Negash, Nur Asyraf Md Akhir, and Luluan Almanna Lubis, 13–22. Springer, Singapore.

Balmforth, Neil J., Ian A. Frigaard, and Guillaume Ovarlez. 2014. Yielding to Stress: Recent Developments in Viscoplastic Fluid Mechanics. *Annual Review of Fluid Mechanics* 46: 121–146. Borghi, G.-P., S Correra, M Merlini, and C Carniani. 2003. Prediction and Scaleup of Waxy Oil Restart Behavior. *International Symposium on Oilfield Chemistry*: 80259.

Cawkwell, M. G., and M. E. Charles. 1987. An improved model for start-up of pipelines containing gelled crude oil. *Journal of Pipelines*.

Davidson, Malcolm R., Q. Dzuy Nguyen, Cheng Chang, and Hans Petter Rønningsen. 2004. A model for restart of a pipeline with compressible gelled waxy crude oil. *Journal of Non-Newtonian Fluid Mechanics* 123: 269–280.

El-Gendy, Husam, Mataz Alcoutlabi, Mark Jemmett, Milind Deo, Jules Magda, Rama Venkatesan, and Alberto Montesi. 2012. The propagation of pressure in a gelled waxy oil pipeline as studied by particle imaging velocimetry. *AIChE Journal* 58: 302–311.

Fossen, Martin, Terje Øyangen, and Ole Jacob Velle. 2013. Effect of the pipe diameter on the restart pressure of a gelled waxy crude Oil. *Energy and Fuels* 27: 3685–3691.

Hénaut, I, O Vincké, and F Brucy. 1999. Waxy Crude Oil Restart : Mechanical Properties of Gelled Oils. *Society of Petrolem Engineers*: 1–7.

Kumar, Lalit, Kistofer Paso, and Johan Sjöblom. 2015. Numerical study of flow restart in the pipeline filled with weakly compressible waxy crude oil in non-isothermal condition. *Journal of Non-Newtonian Fluid Mechanics* 223. Elsevier B.V.: 9–19.

Lee, Hyun Su, Probjot Singh, William H. Thomason, and H. Scott Fogler. 2008. Waxy oil gel breaking mechanisms: Adhesive versus cohesive failure. *Energy and Fuels* 22: 480–487.

Macosko, Christopher W. 1994. *Rheology: Principles, Measurements and Applications*. *Powder Technology*. Vol. 86. Wiley-VCH.

Magda, Jules J., Ahmed Elmadhoun, Peter Wall, Mark Jemmett, Milind D. Deo, Katherine L. Greenhill, and Rama Venkatesan. 2013. Evolution of the pressure profile during the gelation and restart of a model waxy crude oil. *Energy and Fuels* 27: 1909–1913.

Marchesini, Flávio H., Alexandra A. Alicke, Paulo R. De Souza Mendes, and Cláudio M. Ziglio. 2012. Rheological characterization of waxy crude oils: Sample preparation. *Energy and Fuels* 26: 2566–2577.

Oliveira, Gabriel Merhy de, and Cezar O R Negrão. 2015. The effect of compressibility on flow start-up of waxy crude oils. *Journal of Non-Newtonian Fluid Mechanics* 220. Elsevier B.V.: 137–147.

Sanjay, Misra, Baruah Simanta, and Singh Kulwant. 1995. Paraffin Problems in Crude Oil Production And Transportation: A Review. *SPE Production & Facilities* 10: 50–54.

Takamura, Koichi, Herbert Fischer, and Norman R Morrow. 2012. Journal of Petroleum Science and Engineering Physical properties of aqueous glycerol solutions. *Journal of Petroleum Science and Engineering* 98–99. Elsevier: 50–60.

Tarcha, Bruno A., Bárbara P. Bárbara, Edson J. Soares, and Roney L. Thompson. 2015. Critical quantities on the yielding process of waxy crude oils. *Rheologica Acta* 54: 479–499.

Vieira, Lenise Couto. 2008. Estudo do efeito da pressão sobre o fenômeno de cristalização de parafinas de petróleos. UFRJ.

Vinay, Guillaume, Anthony Wachs, and Jean François Agassant. 2006. Numerical simulation of weakly compressible Bingham flows: The restart of pipeline flows of waxy crude oils. *Journal of Non-Newtonian Fluid Mechanics* 136: 93–105.

Wardhaugh, L. T., and D. V. Boger. 1987. Measurement of the unique flow properties of waxy crude oils. *Chemical Engineering Research and Design*.

7. RESPONSIBILITY NOTICE

The authors are the only responsible for the printed material included in this paper.